Research Article

JOURNAL OF HEPATOLOGY

Gas6/Axl pathway is activated in chronic liver disease and its targeting reduces fibrosis via hepatic stellate cell inactivation

Cristina Bárcena[1,2], Milica Stefanovic[1,2], Anna Tutusaus[1,2], Leonel Joannas[3], Anghara Menéndez[2], Carmen García-Ruiz[1,2], Pau Sancho-Bru[1], Montserrat Marí[1,2], Joan Caballeria[1], Carla V. Rothlin[3], José C. Fernández-Checa[1,2,4], Pablo García de Frutos[2,*], Albert Morales[1,2,*]

[1]*Liver Unit, Hospital Clinic, IDIBAPS-CIBEK, CIBEREHD, Barcelona, Catalonia, Spain;* [2]*Department of Cell Death and Proliferation, IIBB-CSIC, Barcelona, Catalonia, Spain;* [3]*Department of Immunobiology, Yale University School of Medicine, New Haven, CT, USA;* [4]*Research Center for Alcoholic Liver and Pancreatic Diseases, Keck School of Medicine of the University of Southern California, Los Angeles, CA, USA*

Background & Aims: Liver fibrosis, an important health concern associated to chronic liver injury that provides a permissive environment for cancer development, is characterized by accumulation of extracellular matrix components mainly derived from activated hepatic stellate cells (HSCs). Axl, a receptor tyrosine kinase and its ligand Gas6, are involved in cell differentiation, immune response and carcinogenesis.

Methods: HSCs were obtained from WT and *Axl*$^{-/-}$ mice, treated with recombinant Gas6 protein (rGas6), Axl siRNAs or the Axl inhibitor BGB324, and analyzed by western blot and real-time PCR. Experimental fibrosis was studied in CCl_4-treated WT and *Axl*$^{-/-}$ mice, and in combination with Axl inhibitor. Gas6 and Axl serum levels were measured in alcoholic liver disease (ALD) and hepatitis C virus (HCV) patients.

Results: In primary mouse HSCs, Gas6 and Axl levels paralleled HSC activation. rGas6 phosphorylated Axl and AKT prior to HSC phenotypic changes, while Axl siRNA silencing reduced HSC activation. Moreover, BGB324 blocked Axl/AKT phosphorylation and diminished HSC activation. In addition, *Axl*$^{-/-}$ mice displayed decreased HSC activation *in vitro* and liver fibrogenesis after chronic damage by CCl_4 administration. Similarly, BGB324 reduced collagen deposition and CCl_4-induced liver fibrosis in mice. Importantly, Gas6 and Axl serum levels increased in ALD and HCV patients, inversely correlating with liver functionality.

Conclusions: The Gas6/Axl axis is required for full HSC activation. Gas6 and Axl serum levels increase in parallel to chronic liver disease progression. Axl targeting may be a therapeutic strategy for liver fibrosis management.

Keywords: Experimental fibrosis; TAM receptors; HSC activation; Chronic liver patients; Gas6/Axl serum levels.

Received 28 October 2014; received in revised form 7 April 2015; accepted 10 April 2015; available online 20 April 2015

* Corresponding authors. Address: Centre Esther Koplowitz, C/ Rosselló 149-153, 4th Floor, 08036 Barcelona, Spain. Tel.: +34 93 2275400x4545; fax: +34 93 3129405.

E-mail addresses: pablo.garcia@iibb.csic.es (P.G. de Frutos), amorales@clinic.ub.es (A. Morales).

Abbreviations: ALD, alcoholic liver disease; COL1A1, Collagen 1A1; ECM, extracellular matrix; HCC, hepatocellular carcinoma; HCV, hepatitis C virus; HSCs, hepatic stellate cells; MMP, matrix metalloproteinase; PCNA, proliferating cell nuclear antigen; ProS, Protein S; rGas6, recombinant Gas6; sAxl, soluble Axl; α-SMA, α-smooth muscle actin; TAM receptor, Tyro3/Axl/MERTK receptor; TGF-β1, transforming growth factor-β1; WT, wild type.

Introduction

Activation of hepatic stellate cells (HSCs) is responsible for the liver fibrosis associated to chronic liver injury of any etiology, being HSCs the main collagen-producing cells in the damaged liver [1,2]. Liver fibrosis, critical pre-stage in the development of liver cirrhosis, may lead to hepatic transplantation or promote a favorable microenvironment for cancer development [3]. HSCs transform during chronic liver injury from a quiescent state into a myofibroblast-like phenotype, which proliferate and migrate towards areas of necrosis and regeneration [4,5]. Activated HSCs alter extracellular matrix (ECM) composition due to the upregulation of proteins such as α-smooth muscle actin (α-SMA), interstitial collagens such as Collagen 1A1 (COL1A1), and matrix metalloproteinases (MMPs) such as MMP9, as well as tissue inhibitor of metalloproteinases (TIMPs), and proteoglycans. Activated HSCs also generate hepatic cytokines such as TGF-β, PDGF, CTGF, FGF, HGF, and VEGF, and recruit inflammatory cells, mono- and polymorphonuclear leukocytes that produce chemokines, including MCP-1, RANTES, CCL21, CCR5. Although HSC critical role in liver fibrosis was proposed a decade ago [6], recent data demonstrates that irrespective of the underlying etiology of liver disease, the majority of myofibroblasts come from the liver-resident HSC population [7]. Moreover, after cessation of the fibrotic triggering insult, around 50% of the activated HSCs survive in an apparently quiescent state, being primed to quickly reactivate into myofibroblasts in response to fibrogenic stimuli [8,9]. Therefore, effective antifibrotic therapies aimed to inhibit activated HSCs, although positive to prevent extracellular matrix deposition, may be insufficient to definitely revert fibrosis, probably requiring the elimination of activated

Molecular and Cell Biology

HSCs for fibrosis resolution in the treatment of chronic liver disease.

Growth arrest-specific gene 6 (*Gas6*) product is a vitamin K-dependent protein that activates a family of receptor tyrosine kinases including Axl, MERTK and Tyro3, known as TAM receptors, whose immunologic and oncogenic properties have been described in detail [10,11]. Among them, Axl receptor signaling has been related to processes leading to cell differentiation and carcinogenesis. Gas6 possesses a high structural homology and sequence identity to the natural anticoagulant protein S (ProS). However, Gas6 and ProS have clearly different biological roles [12,13].

In liver pathologies, a hepatoprotective role for Gas6 has been reported in ischemia/reperfusion-induced damage [14], and in the wound healing response to liver injury [15,16]. In normal liver, Gas6 is mainly expressed in Kupffer cells, while Axl is found in macrophages and in quiescent HSC [17]. Moreover, after acute CCl_4 administration increased Gas6 expression was observed in activated HSCs and macrophages, while Gas6 *in vitro* protection to HSCs was mediated by the Axl/PI3-kinase/AKT pathway [17]. However, the role of Gas6/Axl signaling in chronic liver disease, the potential use of related proteins as serological markers of disease progression, and Gas6/Axl targeting in future liver therapies are aspects that merit further investigation.

To do so, we used both a genetic model of Axl deficiency ($Axl^{-/-}$), and a pharmacologic approach, the Axl inhibitor BGB324 [18]. Our results revealed that Axl receptor is an interesting target to block HSC transformation *in vitro* and demonstrated the efficacy of both strategies, genetic and pharmacologic, to diminish experimental liver fibrosis after chronic administration of CCl_4. Moreover, we analyzed data from patients at different stages of ALD and HCV infection providing evidence of the involvement of the Gas6/Axl axis in human liver fibrosis, and showing the correlation between Gas6/Axl serum levels and liver dysfunction.

In conclusion, our results underscore a critical role of the Gas6/Axl in fibrogenesis and in the progression of chronic liver diseases, suggesting that therapies aimed to inhibit Axl signaling deserve to be undertaken for the treatment of liver fibrosis, particularly now that small molecule inhibitors of Axl have been tested in clinical trials for cancer treatment [19].

Materials and methods

Animal procedures

All procedures were performed according to protocols approved by the Animal Experimentation Ethics Committee from the University of Barcelona. *In vivo* liver fibrogenesis was analyzed after chronic carbon tetrachloride (CCl_4) administration. To this aim, WT or $Axl^{-/-}$ mice were treated with CCl_4 at a dose of 5 μl (10% CCl_4 in corn oil)/g of body weight, by intraperitoneal injection twice a week for five-six weeks. Control animals received corn oil alone. Treatment with Axl inhibitor (BGB324) or vehicle (saline solution) was performed daily for the last ten days of the study via oral gavage at a dose of 80 μg/g body weight. In previous experiments with rodents at similar doses, BGB324 reached serum concentration in the low micromolar range [18], being safe for animal treatment. Control animals received vehicle alone.

HSCs isolation and culture

Wild type and Axl knockout mice livers (male, 8–10 week-old littermates) (C57BL/6 strain) were perfused with collagenase and HSCs cultured as previously described [20,21]. Culture purity, assessed routinely by retinoid autofluorescence at 350 nm, was >95%. Lack of staining for F4/80 confirmed the absence of Kupffer cells. HSCs and LX2 human activated stellate cells [20,22] were cultured in DMEM supplemented with 10% FBS and antibiotics at 37 °C in a humidified atmosphere of 95% air and 5% CO_2. Experiments to compare protein or mRNA content were always performed with cells extracted at the same time of culture, previously treated with recombinant Gas6 (R&D), Axl inhibitor (BGB324, BerGenBio), or siRNA silencing (Santa Cruz) after Lipofectamine 2000 exposure for the indicated periods of time.

SDS-PAGE and immunoblot analysis; RNA isolation and real-time RT-PCR; In Vitro Small Interfering RNA Transfection; Nuclear extract isolation; Immunohistochemical staining; and liver collagen determination

These methods were performed as previously indicated [20,21,23] with modifications as specified in Supplemental methods.

Determination of Gas6, and soluble Axl (sAxl) levels

Measurements of Gas6 and sAxl human levels were carried out using commercial antibodies (R&D Systems) to develop specific ELISAs that use the sandwich technique as described [24]. Serum Gas6 mouse levels were determined using a commercial kit (DuoSet mGas6 ELISA, R&D). Serum sAxl mouse levels were determined by western blot.

Human samples

a) The ALD study group comprised serum samples from 40 individuals: ten healthy normal adult controls (C) and 30 alcoholic patients with different degrees of liver disease as diagnosed after hepatic biopsy and Fibroscan measurement: ten patients with initial fibrosis (Fibroscan score $\leqslant$7 KPa, mean = 5.2 ± 0.4) (F), ten patients with compensated cirrhosis (CH) and, 10 patients with decompensated cirrhosis (DCH), five of them due to ascitis, three due to spontaneous bacterial peritonitis (SBP) and two due to gastrointestinal bleeding by esophageal varices and portal hypertension. Relevant biochemical data are shown in Table 1. b) The HCV study group comprised serum samples from 51 individuals at different stages of liver fibrosis (8 F0, 15 F1, 17 F2, and 11 F3/F4), as stated by liver biopsies, before initiation of treatments. None of the HCV patients exhibited signs of decompensation. Relevant biochemical data are shown in Table 2. All subjects gave written informed consent in accordance with the Declaration of Helsinki, and the protocol, approved by ethical committees from the Hospital Clinic, followed ethical guidelines on handling human samples.

Statistical analyses

Results are expressed as mean ± standard deviation, unless indicated, with the number of individual experiments detailed in Figure legends. Statistical comparisons were performed using unpaired two-tailed Student's *t* test or One-way ANOVA followed by Newman-Keuls Multiple Comparison Test (GraphPad Prism). A *p* value less than 0.05 was considered significant.

Results

TAM receptors and ligands levels during HSC activation

Gas6 and ProS are the ligands of the tyrosine kinase family of receptors named TAM (Tyro3, Axl, and MERTK), which have been involved in numerous processes related to cell transformation and cancer. Since TAM receptor participation in HSC activation has not been explored, we analyzed the presence of transcriptional changes during HSC transdifferentiation in mouse-derived primary cultures of HSCs. A significant increase in the mRNA levels of *Gas6*, but not of *ProS*, was detected (Fig. 1A). In parallel, strong upregulation of Axl was observed, with no significant changes in MERTK levels (Fig. 1B). Tyro3 mRNA levels were not detectable in these samples. Of note, increased secretion of Gas6 protein expression was confirmed in HSCs after different days in culture, as determined by ELISA in 24 h cell conditioned

Table 1. Biochemical data from the ALD patients and control serums analyzed for Gas6 and sAxl levels.

	Cirrhotic decompensated m (9) – f (1)	Cirrhotic compensated m (7) – f (3)	Initial fibrosis m (9) – f (1)	Control values m (6) – f (4)
Age	50.6 ± 6.3	59.2 ± 5.8	48.3 ± 10.1	51.7 ± 10.4
Billirubin (mg/dl)	2.6 ± 3.4 *	1.5 ± 1.5	0.76 ± 0.44	0.2 – 1.0
Albumin (g/L)	31.6 ± 7.2 * #	41.8 ± 4.1	44.5 ± 1.6	35 – 50
Quick (%)	60.2 ± 21.7 * #	76.6 ± 17.2 *	97.9 ± 4.8	70 – 100
MELD	14.7 ± 5.1 * #	10.3 ± 3.7	7.1 ± 1.1	6.43
Creatinin (mg/ml)	0.97 ± 0.26	0.98 ± 0.17	0.81 ± 0.16	0.6 – 1.2
AST (U/L)	47.8 ± 45.0	32.0 ± 9.7	21.5 ± 10.0	10 – 40
ALT (U/L)	22.1 ± 13.1	24.8 ± 7.2	23.0 ± 10.8	10 – 35
GGT (U/L)	106.4 ± 119.0	54.5 ± 38.7	35.4 ± 51.8	5 – 40

For the control group, serums from ten individuals (six males and four females with average age of 51.7 ± 10.4) were used to measure Gas6 and Axl levels. Reference ranges for the each biochemical parameter are provided (right column), as established for normal individuals according to Hospital Clinic Core Lab (Barcelona, Spain). m = male; f = female. $^{*}p \leqslant 0.05$ *vs.* initial fibrosis group (F), $^{\#}p \leqslant 0.05$ *vs.* cirrhotic compensated group (CH). One-way ANOVA, Newman-Keuls Multiple Comparison Test.

Table 2. Biochemical data from the serum of HCV patients analyzed for Gas6 and sAxl levels.

	F0 m (2) – f (6)	F1 m (10) – f (5)	F2 m (11) – f (6)	F3/F4 m (9) – f (2)
Age	41.6 ± 3.8	46.1 ± 2.4	50.2 ± 2.5	53.5 ± 2.8
Billirubin (mg/dl)	0.5 ± 0.1	0.8 ± 0.1	0.9 ± 0.1	1.2 ± 0.2
Albumin (g/L)	44.7 ± 1.2	44.8 ± 0.5	43.8 ± 0.8	41.1 ± 1.3 #
Quick (%)	96.1 ± 2.0	94.4 ± 1.4	90.4 ± 0.7	82.5 ± 3.3 * # &
MELD	7.1 ± 0.3	7.8 ± 0.3	8.4 ± 0.3	9.7 ± 0.6 * #
Creatinin (mg/ml)	1.0 ± 0.1	1.0 ± 0.1	1.0 ± 0.1	1.1 ± 0.1
AST (U/L)	48.3 ± 5.7	48.8 ± 4.7	83.1 ± 14.0	95.5 ± 10.9
ALT (U/L)	74.5 ± 15.9	77.9 ± 10.9	125.5 ± 18.1	108.7 ± 11.9
GGT (U/L)	60.3 ± 13.8	44.2 ± 9.1	70.5 ± 14.1	128.3 ± 44.2

m = male; f = female. $^{*}p \leqslant 0.05$ *vs.* F0 group. $^{\#}p \leqslant 0.05$ *vs.* F1 group. $^{\&}p \leqslant 0.05$ *vs.* F2 group. One-way ANOVA, Newman-Keuls Multiple Comparison Test.

medium (Fig. 1C). Thus, the activation of WT HSCs is paralleled by an increase in expression of Axl, and the expression and secretion into the medium of Gas6.

Axl is required for full HSC activation and proliferation in vitro

To verify the repercussion of this correlation in HSC transformation, we analyzed the effect of reducing the expression of Axl in activated HSCs, by means of RNA silencing, and the consequences of Gas6 supplementation. Since primary HSCs are not easy to manipulate genetically, we used the LX2 human activated HSC cell line. LX2 cells with depleted Axl levels by siRNA transfection displayed a significant reduction in α-SMA levels (Fig. 2A). Moreover, we tested if recombinant Gas6 (rGas6) may further increase LX2 cells activation, and observed enhanced levels of α-SMA in LX2 exposed to rGas6 for up to three days (Fig. 2B), compared to cells treated with vehicle (PBS). In addition, rGas6 administration induced a fast Axl and AKT phosphorylation in LX2 cells (Fig. 2C). Of note, Gas6-dependent AKT activation was responsible for the nuclear translocation of the anti-apoptotic NF-κB subunit p65, since it was detected in nuclear extracts of LX2 cells immediately after rGas6 administration, while PI3K inhibitor LY294002 blocked p65 nuclear upregulation. These results, in line with previous observations in activated HSCs [17], supported the participation of Gas6 activation on the proliferation and survival of HSCs via the AKT/NF-κB signaling pathways. However, since we also observed that rGas6 phosphorylated MERTK (Fig. 2C), at this point we cannot discard a potential role of MERTK in HSC signaling.

To better examine Axl contribution, HSCs from $Axl^{-/-}$ mice were obtained, cultured and analyzed in comparison to WT HSCs. A significant reduction in the mRNA levels of the markers for HSC activation α-SMA and Col1a1 was observed in Axl deficient mice, as well as in TIMP-1 mRNA, while no differences for TGF-β levels were detected (Fig. 2D). Indeed, $Axl^{-/-}$ HSCs showed decreased protein levels of α-SMA *in vitro*, showing a reduced activation state after 10 days and delayed proliferation, as manifested by MMP9 and PCNA levels, respectively (Fig. 2E). Although not all the variety of proteins induced during HSC activation are affected by Axl, as the absence of changes in TGF-β seem to indicate, taken as a whole, these results suggest that Axl signaling is required for full activation of HSCs *in vitro*.

Axl deficiency diminished liver fibrosis induced by carbon tetrachloride

To investigate if Gas6/Axl role in HSC activation *in vitro* may reflect a key participation of this system in the development of liver fibrosis, we used the chronic administration of CCl_4 as a model to generate liver damage and fibrogenesis in mice. First,

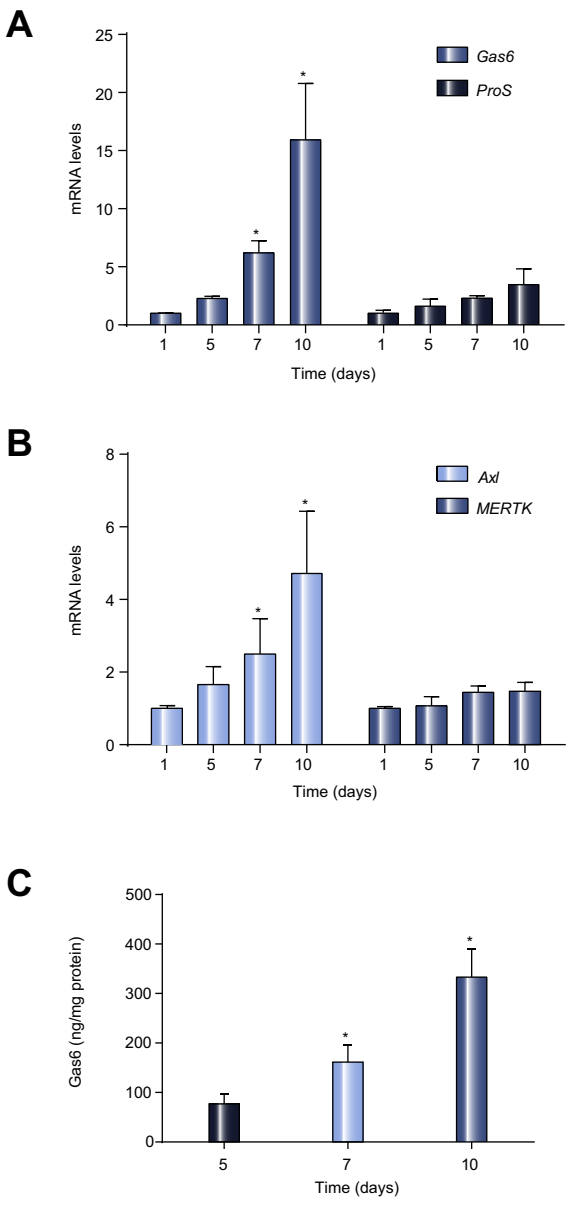

Fig. 1. Gas6 and Axl levels are increased in WT HSCs during *in vitro* activation. (A and B) mRNA expression level of *Gas6*, *ProS*, *Axl*, and *MERTK* in HSCs at different times of *in vitro* activation, using β-actin as control. (n ⩾3). (C) Gas6 protein levels released to fresh culture medium during 24 h from HSCs at different time points of *in vitro* activation, detected by ELISA and corrected by cellular protein content. (n = 3). $^{*}p \leqslant 0.05$, Student's *t* test.

we wanted to analyze if Gas6 and Axl levels are modified in animals suffering liver fibrosis. After five weeks of CCl_4 treatment mice exhibited increased Gas6 and sAxl serum levels compared to oil-treated animals (Fig. 3A), indicating that this pathway is upregulated during CCl_4-induced liver fibrosis. Second, we analyzed in $Axl^{-/-}$ mice the effect of CCl_4 administration. After five weeks, liver hydroxyproline levels, indicative of collagen deposition, were significantly lower in Axl deficient animals treated with CCl_4 (Fig. 3B), suggesting reduced liver fibrosis as confirmed in liver sections after Sirius Red staining and quantification (Fig. 3C and D). In accordance, liver homogenates exhibited an increase in α-SMA and MMP9 after CCl_4 administration that was reduced in $Axl^{-/-}$ mice (Fig. 3E) indicative of HSC activation and changes in ECM composition. Analogously, α-SMA stained liver slides from CCl_4-treated $Axl^{-/-}$ mice exhibited similar reduction (Supplementary Fig. 1A). Finally, we checked the degree of liver injury to verify that the lower liver fibrosis observed in $Axl^{-/-}$ mice is not a consequence of reduced hepatocellular damage induced by CCl_4. Both WT and Axl deficient mice displayed similar ALT levels after CCl_4 exposure, which allows discarding reduced liver fibrosis as a consequence of lesser hepatic damage.

It has been proposed that Gas6 deficiency could lead to a decline in liver fibrosis after CCl_4 exposure due to reduced macrophage recruitment [25]. Therefore, we decided to analyze potential differences in liver inflammation and immune cell recruitment to the liver. When we quantified the mRNA levels of inflammatory cytokines (TNF), chemokines (MCP-1) or neutrophil infiltration (MPO) in WT and $Axl^{-/-}$ CCl_4-treated mice they were similarly increased, as compared to their untreated controls (Supplementary Fig. 1B and D). In addition, no changes in MPO staining were observed between WT and $Axl^{-/-}$ CCl_4-treated animals (Supplementary Fig. 1C). However, a minor level of macrophages (F4/80) and newly-recruited monocytes/-macrophages (CCR2) were detected in the livers of Axl deficient mice after CCl_4 exposure (Supplementary Fig. 1D). These results support a role for the Gas6/Axl pathway in macrophage response to CCl_4 exposure, as previously indicated [25], and are in line with other models of tissue damage such as advanced atherosclerotic plaques in GAS6 deficient animals [26].

BGB324, small molecule inhibitor of Axl, blocks HSC activation in vitro and reduces CCl_4-induced liver fibrosis in WT mice

Axl is an attractive target for the treatment of different human pathologies, particularly in cancer. Interestingly, a small molecule inhibitor of Axl (BGB324, BerGenBio) has entered clinical trials for cancer treatment. We tested the effect of BGB324 administration for 24 h on seven-day old WT HSC cells (Fig. 4A). Axl inhibitor administration was able to reduce the activation of primary HSCs, even inducing HSC elimination at higher doses in the micromolar range (Fig. 4A, upper image). This effect was specific for Axl inhibition since BGB324 administration did not affect MERTK phosphorylation (Fig. 4A, lower image), while effectively blocked AKT activation after short-term incubation with rGas6 (30 min., 200 ng/ml) (Fig. 4B).

To analyze whether inhibition of Axl, using BGB324, may play a role in the progression of liver fibrogenesis, mice were injected CCl_4 twice weekly to stimulate HSC activation and promote liver fibrosis. After four weeks, animals started receiving BGB324 co-treatment via oral gavage on a daily basis for ten additional days. Determination of the hepatic hydroxyproline content showed a significant decrease in the accumulation of collagen fibers in animals treated with CCl_4 that received Axl inhibitor compared to control animals (Fig. 4C). This result was confirmed after Sirius Red staining, showing less deposition of collagen fibers in animals treated with BGB324 and CCl_4, compared to CCl_4-vehicle treated mice (Fig. 4D), as denoted by the quantification of collagen content in different sections (Fig. 4E). Moreover, mice that received BGB324 exhibited reduced levels of MMP9 and α-SMA after CCl_4 exposure (Supplementary Fig. 2A), and diminished α-SMA staining in liver slides compared to CCl_4-treated mice without inhibitor administration (Supplementary Fig. 2B), confirming changes in ECM composition

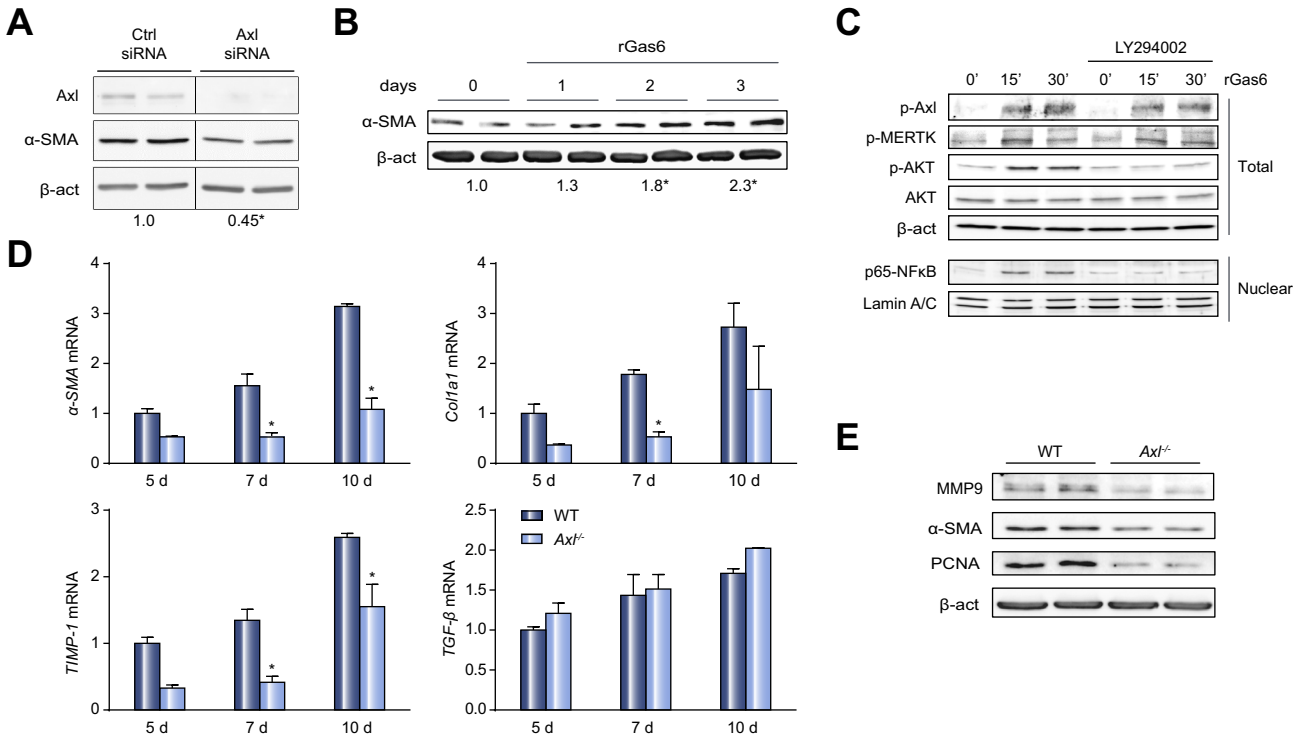

Fig. 2. Recombinant Gas6 induces HSC activation via Axl/AKT signaling and Axl deficiency reduces specific traits of HSC transdifferentiation. (A) *Axl* silencing using specific siRNAs reduced Axl protein expression and HSC activation, quantified as the ratio α-SMA/β-actin at 48 h post-transfection. (n = 3). (B) Representative western blot of α-SMA expression in LX2 treated with rGas6 (500 ng/ml) for 0 to 3 days and quantification compared to β-actin content. (n = 2). (C) Representative western blot of phospho-Axl, phospho-MERTK, phospho-AKT, AKT and β-actin in total extracts, and p65 subunit of NF-κB and laminin in nuclear extracts from LX2 cells after rGas6 administration (500 ng/ml) and incubation with PI3K inhibitor LY294002. (n = 2). (D) mRNA expression level of α-*SMA*, *Col1a1*, *TIMP-1*, and *TGF-β* in HSCs from WT and *Axl*$^{-/-}$ mice cultured *in vitro* for different times, using as β-actin control (n = 3). (E) Representative western blot of α-SMA, PCNA and MMP9 in protein extracts from WT and *Axl*$^{-/-}$ mice HSCs after ten days of *in vitro* culture (n = 2). $^{*}p \leqslant 0.05$, Student's *t* test.

and HSC activation. Of note, serum levels of ALT after CCl_4 administration were similar in vehicle and Axl inhibitor-treated mice indicating that the antifibrotic effect of BGB324 is not a consequence of reduced hepatocellular damage after chemical exposure (Fig. 4F).

Interestingly, when we analyzed changes in liver inflammation and immune cell recruitment to the liver induced by BGB324, we obtained results in accordance with the data provided by the *Axl*$^{-/-}$ mice. While a comparable degree of TNF, MCP-1 or neutrophil infiltration was observed in all CCl_4-treated mice (Supplementary Fig. 2C and D), animals that received BGB324 exhibited decreased macrophage recruitment (Supplementary Fig. 2D), in line with previous results observed analyzing Gas6 KO mice [25].

Serum levels of Gas6 and sAxl correlate with liver dysfunction in human ALD, and increased during HCV-induced fibrosis progression

Serum levels of Gas6 and/or sAxl have been related to cancer prognosis and to other pathologies, such as heart failure or sepsis [27,28]. Since our results point to Gas6/Axl axis as a relevant signaling pathway in liver fibrogenesis, we decided to evaluate this pathway in patients with different degrees of ALD in which progression from asymptomatic fibrosis to decompensated cirrhosis is a well-studied process [29]. Therefore, we determined Gas6 and sAxl concentration in serum samples from alcoholic patients in initial (F0/F1) stages of liver fibrosis (F), patients with compensated (CH), and patients with decompensated hepatic cirrhosis (DCH), and compared them to control individuals (C). Both Gas6 and sAxl were found increased in serum levels of cirrhotic patients, showing close correlation with the severity of the disease, although behaving differently. Specifically, sAxl concentration was already augmented in individuals with compensated cirrhosis compared to initial fibrosis (Fig. 5B), while Gas6 levels were increased markedly in the DCH group (Fig. 5A).

To verify this observation, we examined the relationship between the serum levels of Gas6 and sAxl compared to the Model for End-Stage Liver Disease (MELD) score system, which assigns a value calculated from different biochemical parameters altered in chronic liver disease. The analysis revealed a remarkable correlation between the MELD score and both proteins (Fig. 5C and D), being better for Gas6 serum levels ($r^2 = 0.78$). Interestingly, we identified an algorithm containing sAxl and Gas6 that can achieve even stronger correlation ($r^2 = 0.86$) with the MELD score (Fig. 5D), suggesting that the measurement of both proteins provides a better evaluation of liver functionality.

However, since our ALD group contains only individuals with early F0/F1 fibrosis and with cirrhosis, compensated or decompensated, our measurements did not allow to verify an increase in the Gas6/Axl system during the progression of fibrosis, or to validate Gas6/Axl detection in other human hepatic pathologies. To do so, we analyzed Gas6 and sAxl levels in the serum of HCV patients at different stages of liver fibrosis before starting treatments (Fig. 5E and F). Our data revealed that Gas6 levels were significantly different between individual with established fibrosis (F2) and patients with initial fibrosis (F0 and F1 groups).

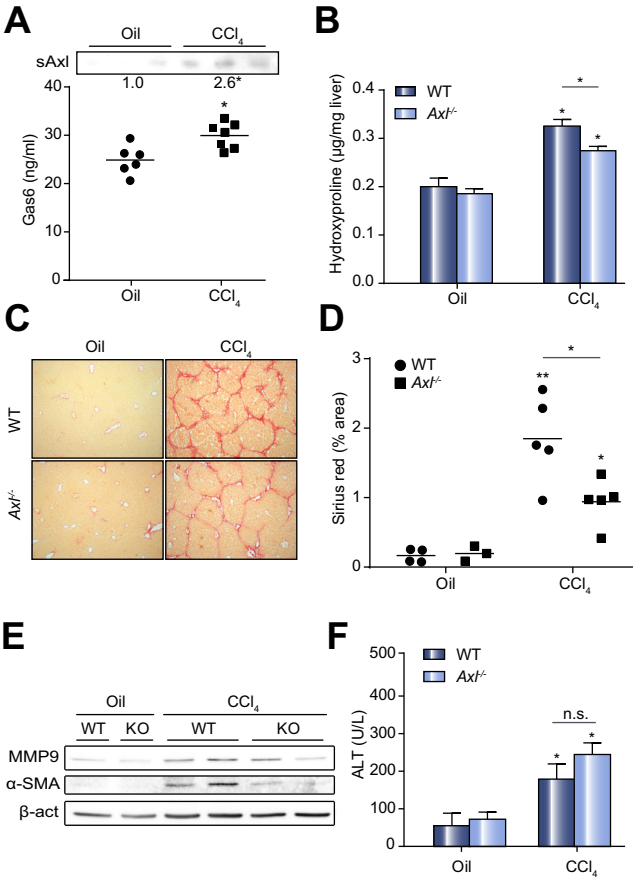

Fig. 3. Gas6/Axl pathway is activated in CCl_4-treated mice and Axl deficiency reduces CCl_4-induced liver fibrosis. WT and $Axl^{-/-}$ mice were i.p. treated with CCl_4 (twice a week) for five weeks. (A) Gas6 and Axl levels in serum from WT mice treated with CCl_4 or vehicle (corn oil). Additionally, in WT and $Axl^{-/-}$ mice treated with CCl_4 or vehicle were measured: (B) Hydroxyproline levels in liver extracts. (C) Representative images of liver sections after Sirius Red staining (20×). (B) Sirius Red quantification of liver slides using Quantity One software in four random sections from each animal. (E) Representative western blot of α-SMA, and MMP9 in liver extracts. (E) ALT serum levels. $^{*}p \leqslant 0.05$, $^{**}p \leqslant 0.01$ *vs.* untreated WT mice, unless indicated. (This figure appears in colour on the web.)

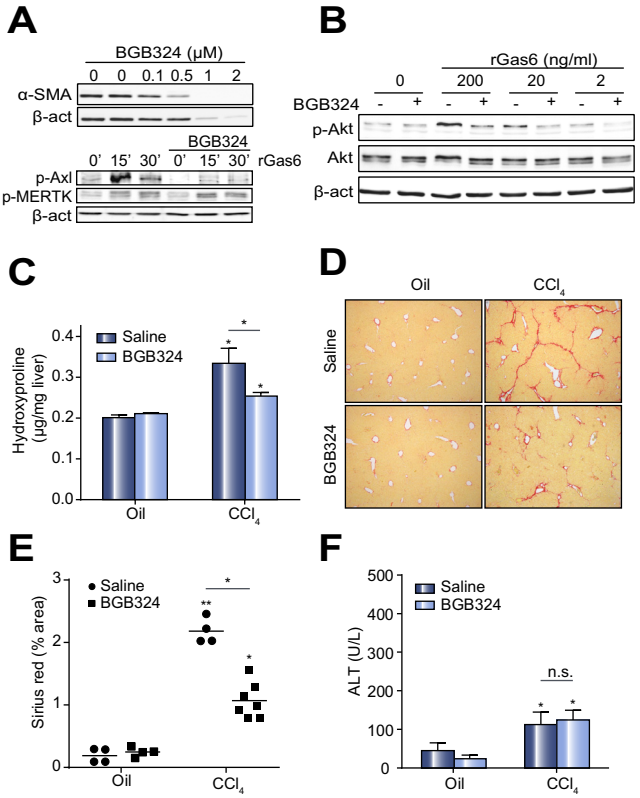

Fig. 4. Axl inhibitor BGB324 reduces HSC activation *in vitro* and liver fibrosis in CCl_4-treated mice. (A) Representative western blot of α-SMA expression in cell extract from WT HSCs treated with BGB324 (0–2 μM) for 24 h or vehicle (lanes 1 and 2) in upper image; and phospho-Axl, phospho-MERTK, and β-actin in total extracts, from LX2 cells after rGas6 administration (500 ng/ml) and BGB324 pre-incubation (30 min, 1 μM) in lower image (n = 3). (B) phospho-AKT, AKT and α-SMA expression in LX2 cells pre-treated with BGB324 (30 min, 1 μM) before administration of different doses of rGas6 for 30 min. (n = 2). (C) Hydroxyproline levels in liver extracts from WT mice treated with CCl_4 or vehicle that received BGB324 (80 mg/kg, oral gavage, daily) or vehicle. (D) Representative images of liver sections after Sirius Red staining (20×) from mice treated as above. (E) Sirius Red quantification of liver slides. (F) ALT serum levels from mice i.p. treated with CCl_4 or vehicle that received Axl inhibitor or saline by oral gavage. $^{*}p \leqslant 0.05$, $^{**}p \leqslant 0.01$ *vs.* untreated WT mice, unless indicated. (This figure appears in colour on the web.)

In addition, sAxl levels displayed significant changes between patients with F2 fibrosis and individuals with advanced fibrosis or cirrhosis (F3/F4 group). These findings underscore the relevance of the Gas6/Axl pathway during the development of ALD- and HCV-induced liver damage, supporting Gas6 and sAxl serum levels as indicative parameters of hepatic dysfunction and fibrosis development in liver disease.

Discussion

HSC transdifferentiation represents a crucial cell reprogramming event that shifts HSCs from a normal vitamin A-storing to an ECM-remodeling phenotype that favors tumorigenic development [4]. Despite recent progress in understanding the biology of HSCs, the mechanisms are not yet fully known. In fact, besides the treatment/withdrawal of the underlying cause, fibrosis regression in chronic liver diseases is not accomplished by any antifibrotic drug despite the experimental description of an array of pharmacological targets [1,5]. In this context, the characterization of the role of Gas6/Axl pathway in liver fibrosis, by participating in the activation of HSC may provide a new therapeutic target, not only for liver fibrosis, but also for different chronic liver diseases. Moreover, the existence of specific Axl inhibitors [30], already in clinical trials, may facilitate the biomedical translation of our results (Fig. 6).

Here, we used BGB324 (BerGenBio), an inhibitor of Axl ready to reach Phase Ib clinical trials for cancer treatment after showing good tolerability by healthy volunteers in doses up to 1.5 g/daily with a long plasma half-life [31]. BGB324 is highly specific for Axl inhibition, having exhibited >100-fold selectivity for Axl *vs.* Abl and 50- and >100-fold selectivity over TAM family kinases MERTK and Tyro3, respectively, in cells-based assays [18]. In fact, we observed that at doses effective to block AKT phosphorylation and HSC activation, BGB324 did not alter MERTK phosphorylation by rGas6. Although, based in our data, we cannot discard other off-target effects of BGB324 administration, the highly

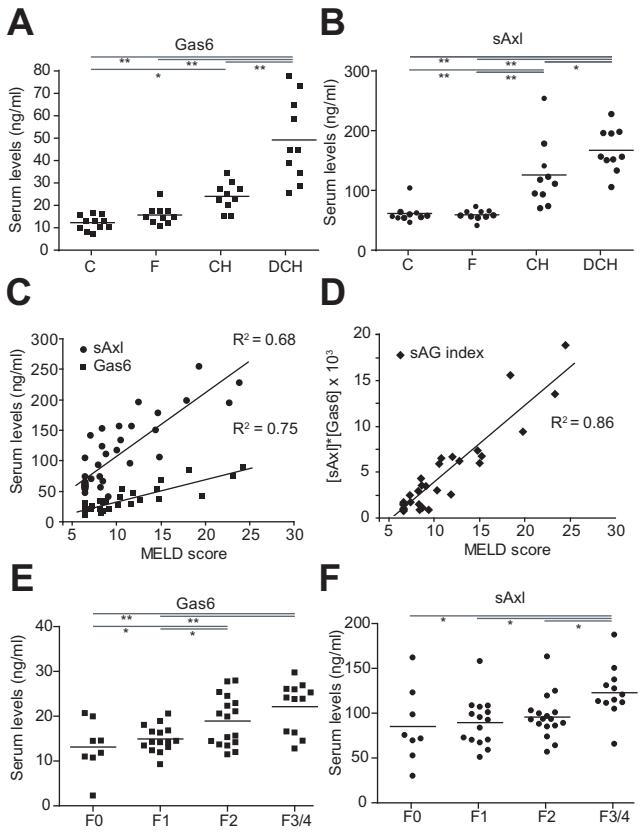

Fig. 5. Gas6 and sAxl serum levels are increased in alcoholic liver disease (ALD) and HCV-infected patients. (A) Gas6 and (B) Axl serum levels were measured in control individuals and patients with liver disease associated to alcohol consumption. Groups: (C) control, (F) initial liver fibrosis (F0/F1), CH, hepatic cirrhosis, and DCH, decompensated hepatic cirrhosis. Additional data of patients is provided in Table 1. $^{*}p \leqslant 0.05$, $^{**}p \leqslant 0.001$ between groups. One-way ANOVA, Newman-Keuls Multiple Comparison Test. (C) Correlation analysis between Gas6/sAxl and MELD score was calculated for all the ALD patients (n = 30). (D) sAG index, an algorithm calculated by multiplication of sAxl and Gas6 concentrations is plotted against MELD index. (E) Gas6 and (F) Axl serum levels were measured in HCV patients with different fibrosis staging. Groups: F0 (no fibrosis), F1 (mild), F2 (moderate), and F3/F4 (severe fibrosis/cirrhosis). $^{*}p \leqslant 0.05$, $^{**}p \leqslant 0.01$ between groups. One-way ANOVA, Newman-Keuls Multiple Comparison Test.

similar results obtained between the *Axl*$^{-/-}$ mice and the BGB324-treated mice suggest that the anti-fibrotic action of BGB324 is mainly due to Axl inhibition.

High levels of Axl expression have been observed in many types of cancer correlating with poor survival; among them glioblastoma multiforme [32], acute myeloid leukemia [33], breast cancer [34], osteosarcoma [35] and renal cell carcinoma [36]. Moreover, Axl activation is a mechanism of drug resistance to therapies targeting EGFR mechanism in lung cancer [37]. However, Axl and MERTK are also expressed by macrophages and dendritic cells, where they limit excessive immune response [10,38]. This aspect has raised concerns and could limit the use of TAM receptors as targets in cancer, in special since blockage of Axl/ MERTK promote the development of tumor growth in an inflammatory environment such as colon cancer [39], a tumor that benefits of a pro-inflammatory milieu similarly as liver cancer does. Importantly, this deleterious effect seems to require the simultaneous absence of both kinases (Axl and MERTK) activities [40], and BGB324 is already effective at doses that provide serum

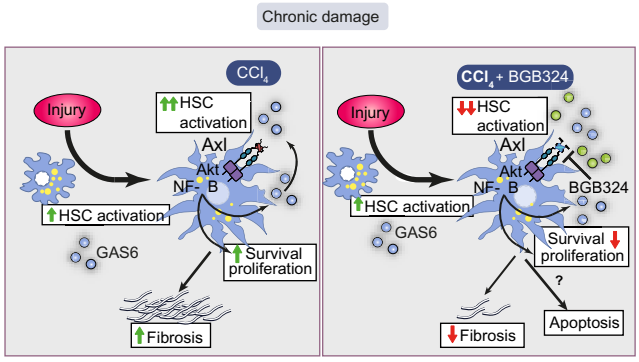

Fig. 6. Schematic representation of Gas6/Axl role in liver fibrosis induced by chronic damage. In a mouse model of chemical-induced liver fibrosis Gas6/Axl signaling is induced. Increased Gas6 extracellular levels stimulate Axl activation in HSCs leading to HSC proliferation and phenotypic transformation via AKT phosphorylation and NF-κB nuclear translocation. Axl genetic deficiency (*Axl*$^{-/-}$ mice) or Axl inhibition by BGB324 blocks fibrogenesis, effectively inhibiting Gas6-induced HSC activation *in vitro* and reducing experimental liver fibrosis *in vivo* by eliminating activated HSCs. Therefore, small molecule inhibitors of Axl may be interesting compounds for the medical treatment of chronic liver fibrosis and prevention of HCC development. (This figure appears in colour on the web.)

concentration in the low micromolar range, with minimal affinity for MERTK [18]. This observation is supported by our results in mice, not having detected inflammation in treated animals, displaying similar levels of neutrophil infiltration after CCl_4 administration. In fact, BGB324 has just received orphan-drug designation from FDA in the treatment of acute myeloid leukemia, supporting its good tolerability and lack of side-effects in clinical trials. In this sense, BGB324 accomplished a feature required to Axl inhibitors for systemic administration in cancer, particularly for hepatocellular carcinoma, to act without favoring a pro-carcinogenic background. Of note, other approaches to block Axl signaling are already under study, for instance an Axl 'decoy receptor' has been recently engineered, showing capacity to inhibit metastasis and cancer progression *in vivo* [40]. Therefore, BGB324 and other molecules that antagonize the Gas6/Axl pathway deserve to be further analyzed in the context of advanced liver fibrosis, and most probably of liver cancer development.

Several reports have positioned Gas6 as a protective molecule against ischemia/reperfusion [14] and promoter of liver regeneration after acute liver damage [15,16], while its deficiency was associated to decreased liver fibrosis [25]. We considered using Gas6 KO mice to analyze Gas6/Axl system in HSC activation but previous results showing compensatory alterations such as Axl overexpression in the liver [25], refrained us to do it. In fact, we verified in murine *Gas6*$^{-/-}$ HSCs high expression of Axl, increased AKT phosphorylation, and elevated α-SMA levels, among other markers of HSC activation (Supplementary Fig. 3). Since Gas6/Axl axis is not blocked in *Gas6*$^{-/-}$ HSCs, we preferred to use the *Axl*$^{-/-}$ mouse model instead. In this sense, our data targeting directly Axl underscore the importance of Gas6/Axl pathway in liver disease, being supported by similar results obtained after administration of the small molecule inhibitor BGB324.

Although it has been reported an increase in Gas6/Axl proteins in patients with hepatocellular carcinoma from different etiologies [41], and sAxl levels are increased in end-stage heart failure patients undergoing heart transplantation [27], which

frequently suffer cardiac fibrosis, Gas6/Axl as serological markers of liver function have not been previously proposed. We have confirmed in serum samples from ALD and HCV patients an enhancement in Gas6 and sAxl serum levels. Although we can not discard that the prominent increase in Gas6/Axl observed in these ALD cirrhotic patients may be partially due to a deficient liver protein clearance, the observation that a similar increase is also detected in fibrotic HCV patients, even in patients without cirrhosis, suggests otherwise. Moreover, an algorithm combination of Gas6 and sAxl levels display an excellent correlation with the degree of liver dysfunction in ALD patients determined by the MELD index ($r^2 = 0.86$ for sAG index) suggesting that the measurement of both proteins provides additional information to analyze liver functionality. In this sense, we consider that preclinical research may also benefit from Gas6/Axl levels to measure fibrosis progression, since numerous targets for antifibrotic agents have problems to be analyzed or to enter early-phase clinical studies due to the lack of sensitive markers to follow the effects [42]. These results point to Gas6/sAxl determination as a significant diagnostic tool for chronic liver disease, and help us to position Gas6/Axl signaling pathway as a relevant in human liver pathology.

In conclusion, Gas6/Axl is a profibrogenic route that is activated in patients with chronic liver disease. Therefore, small molecule inhibitors against Axl, that effectively eliminate HSC activation and reduce experimental fibrosis progression, may be an interesting therapeutic tool for future clinical trials.

Financial support

This study was funded by grants from the Instituto de Salud Carlos III (FIS PI12/00110, PI09/00056 to A.M., FIS PI13/00374 to M.M., PI12/01265 to J.C., PI14/00320 to P.S-B. and PI11/0325 to J.F.C.), Ministerio de Economía y Competitividad (BFU2010-22185 to P.G.F., SAF2012/34831 to J.F.C. and SAF2011-23031 to C.G.R.) and co-funded by FEDER (Fondo Europeo de Desarrollo Regional, Unión Europea. "Una manera de hacer Europa"); center grant P50-AA-11999 from Research Center for Liver and Pancreatic Diseases, (US NIAAA to J.F.C.); National Institutes of Health (R01 AI089824 to C.V.R); Fundació la Marató de TV3 to J.F.C.; Fundación Mutua Madrileña (AP103502012 to C.G.R.) and by CIBERehd from the Instituto de Salud Carlos III.

Conflict of interest

P.G.F. is inventor on a patent filed for use of sAxl for diagnosis/prognosis of heart failure syndrome (E.U. patent number EP 13703603.4). Other authors declare no competing interests.

Author's contributions

C.B., M.S., A.T., L.J., L.M., and An.M. performed the experiments; C.G.R., P.S-B., and J.C. analyzed clinical data and discussed the results; C.B. drafted the manuscript; J.F.C., M.M., C.V.R., P.G.F., and A.M. designed experiments and revised the results; P.G.F. and A.M. were primarily responsible for writing the manuscript. All authors contributed to manuscript editing and approval.

Acknowledgements

Authors are grateful to Guillermo A. Martinez-Nieto and Susana Nuñez for her technical support and Dr. Anna Colell for her insightful comments. We are greatly indebted to BerGenBio AS (Norway) for the gift of Axl inhibitor BGB324. Most of the work of this study was carried out at the Esther Koplowitz Center (CEK).

Supplementary data

Supplementary data associated with this article can be found, in the online version, at http://dx.doi.org/10.1016/j.jhep.2015.04.013.

References

Authors names in bold designate shared co-first authorship.

[1] Mallat A, Lotersztajn S. Cellular mechanisms of tissue fibrosis. 5. Novel insights into liver fibrosis. Am J Physiol Cell Physiol 2013;305:C789–C799.
[2] Bataller R, Brenner DA. Liver fibrosis. J Clin Invest 2005;115:209–218.
[3] Coulouarn C, Corlu A, Glaise D, Guenon I, Thorgeirsson SS, Clement B. Hepatocyte-stellate cell cross-talk in the liver engenders a permissive inflammatory microenvironment that drives progression in hepatocellular carcinoma. Cancer Res 2012;72:2533–2542.
[4] Friedman SL. Hepatic stellate cells: protean, multifunctional, and enigmatic cells of the liver. Physiol Rev 2008;88:125–172.
[5] Friedman SL, Sheppard D, Duffield JS, Violette S. Therapy for fibrotic diseases: nearing the starting line. Sci Transl Med 2013;5:167sr1.
[6] Bataller R, Brenner DA. Hepatic stellate cells as a target for the treatment of liver fibrosis. Semin Liver Dis 2001;21:437–451.
[7] Mederacke I, Hsu CC, Troeger JS, Huebener P, Mu X, Dapito DH, et al. Fate tracing reveals hepatic stellate cells as dominant contributors to liver fibrosis independent of its aetiology. Nat Commun 2013;4:2823.
[8] **Troeger JS**, **Mederacke I**, Gwak GY, Dapito DH, Mu X, Hsu CC, et al. Deactivation of hepatic stellate cells during liver fibrosis resolution in mice. Gastroenterology 2012;143:e22.
[9] Kisseleva T, Cong M, Paik Y, Scholten D, Jiang C, Benner C, et al. Myofibroblasts revert to an inactive phenotype during regression of liver fibrosis. Proc Natl Acad Sci U S A 2012;109:9448–9453.
[10] Lemke G, Rothlin CV. Immunobiology of the TAM receptors. Nat Rev Immunol 2008;8:327–336.
[11] Linger RM, Keating AK, Earp HS, Graham DK. TAM receptor tyrosine kinases: biologic functions, signaling, and potential therapeutic targeting in human cancer. Adv Cancer Res 2008;100:35–83.
[12] Bellido-Martin L, de Frutos PG. Vitamin K-dependent actions of Gas6. Vitam Horm 2008;78:185–209.
[13] Fernandez-Fernandez L, Bellido-Martin L, Garcia de Frutos P. Growth arrest-specific gene 6 (GAS6). An outline of its role in haemostasis and inflammation. Thromb Haemost 2008;100:604–610.
[14] **Llacuna L**, **Barcena C**, Bellido-Martin L, Fernandez L, Stefanovic M, Mari M, et al. Growth arrest-specific protein 6 is hepatoprotective against murine ischemia/reperfusion injury. Hepatology 2010;52:1371–1379.
[15] Couchie D, Lafdil F, Martin-Garcia N, Laperche Y, Zafrani ES, Mavier P. Expression and role of Gas6 protein and of its receptor Axl in hepatic regeneration from oval cells in the rat. Gastroenterology 2005;129:1633–1642.
[16] Lafdil F, Chobert MN, Deveaux V, Zafrani ES, Mavier P, Nakano T, et al. Growth arrest-specific protein 6 deficiency impairs liver tissue repair after acute toxic hepatitis in mice. J Hepatol 2009;51:55–66.
[17] Lafdil F, Chobert MN, Couchie D, Brouillet A, Zafrani ES, Mavier P, et al. Induction of Gas6 protein in CCl4-induced rat liver injury and anti-apoptotic effect on hepatic stellate cells. Hepatology 2006;44:228–239.
[18] Holland SJ, Pan A, Franci C, Hu Y, Chang B, Li W, et al. R428, a selective small molecule inhibitor of Axl kinase, blocks tumor spread and prolongs survival in models of metastatic breast cancer. Cancer Res 2010;70:1544–1554.

[19] Sheridan C. First Axl inhibitor enters clinical trials. Nat Biotechnol 2013;31:775–776.
[20] **Moles A**, **Tarrats N**, Fernandez-Checa JC, Mari M. Cathepsin B overexpression due to acid sphingomyelinase ablation promotes liver fibrosis in Niemann-Pick disease. J Biol Chem 2012;287:1178–1188.
[21] Tarrats N, Moles A, Morales A, Garcia-Ruiz C, Fernandez-Checa JC, Mari M. Critical role of tumor necrosis factor receptor 1, but not 2, in hepatic stellate cell proliferation, extracellular matrix remodeling, and liver fibrogenesis. Hepatology 2011;54:319–327.
[22] Xu L, Hui AY, Albanis E, Arthur MJ, O'Byrne SM, Blaner WS, et al. Human hepatic stellate cell lines, LX-1 and LX-2: new tools for analysis of hepatic fibrosis. Gut 2005;54:142–151.
[23] Moles A, Tarrats N, Morales A, Dominguez M, Bataller R, Caballeria J, et al. Acidic sphingomyelinase controls hepatic stellate cell activation and in vivo liver fibrogenesis. Am J Pathol 2010;177:1214–1224.
[24] **Recarte-Pelz P**, **Tassies D**, Espinosa G, Hurtado B, Sala N, Cervera R, et al. Vitamin K-dependent proteins GAS6 and Protein S and TAM receptors in patients of systemic lupus erythematosus: correlation with common genetic variants and disease activity. Arthritis Res Ther 2013;15:R41.
[25] Fourcot A, Couchie D, Chobert MN, Zafrani ES, Mavier P, Laperche Y, et al. Gas6 deficiency prevents liver inflammation, steatohepatitis, and fibrosis in mice. Am J Physiol Gastrointest Liver Physiol 2011;300:G1043–G1053.
[26] **Lutgens E**, **Tjwa M**, Garcia de Frutos P, Wijnands E, Beckers L, Dahlbäck B, et al. Genetic loss of Gas6 induces plaque stability in experimental atherosclerosis. J Pathol 2008;216:55–63.
[27] **Batlle M**, **Recarte-Pelz P**, Roig E, Castel MA, Cardona M, Farrero M, et al. AXL receptor tyrosine kinase is increased in patients with heart failure. Int J Cardiol 2014;173:402–409.
[28] Ekman C, Linder A, Akesson P, Dahlback B. Plasma concentrations of Gas6 (growth arrest specific protein 6) and its soluble tyrosine kinase receptor sAxl in sepsis and systemic inflammatory response syndromes. Crit Care 2010;14:R158.
[29] Altamirano J, Bataller R. Alcoholic liver disease: pathogenesis and new targets for therapy. Nat Rev Gastroenterol Hepatol 2011;8:491–501.
[30] Wnuk-Lipinska K, Gausdal G, Sandal T, Frink R, Hinz S, Hellesøy M, et al. BGB324, a selective small molecule Axl kinase inhibitor to overcome EMT-associated drug resistance in carcinomas: Therapeutic rationale and early clinical studies. San Diego, CA: AACR; 2014.
[31] Feneyrolles C, Spenlinhauer A, Guiet L, Fauvel B, Dayde-Cazals B, Warnault P, et al. Axl kinase as a key target for oncology: focus on small molecule inhibitors. Mol Cancer Ther 2014;13:2141–2148.
[32] **Hutterer M**, **Knyazev P**, Abate A, Reschke M, Maier H, Stefanova N, et al. Axl and growth arrest-specific gene 6 are frequently overexpressed in human gliomas and predict poor prognosis in patients with glioblastoma multiforme. Clin Cancer Res 2008;14:130–138.
[33] **Ben-Batalla I**, **Schultze A**, Wroblewski M, Erdmann R, Heuser M, Waizenegger JS, et al. Axl, a prognostic and therapeutic target in acute myeloid leukemia mediates paracrine crosstalk of leukemia cells with bone marrow stroma. Blood 2013;122:2443–2452.
[34] **Gjerdrum C**, **Tiron C**, **Hoiby T**, Stefansson I, Haugen H, Sandal T, et al. Axl is an essential epithelial-to-mesenchymal transition-induced regulator of breast cancer metastasis and patient survival. Proc Natl Acad Sci U S A 2010;107:1124–1129.
[35] **Han J**, **Tian R**, Yong B, Luo C, Tan P, Shen J, et al. Gas6/Axl mediates tumor cell apoptosis, migration and invasion and predicts the clinical outcome of osteosarcoma patients. Biochem Biophys Res Commun 2013;435:493–500.
[36] Gustafsson A, Martuszewska D, Johansson M, Ekman C, Hafizi S, Ljungberg B, et al. Differential expression of Axl and Gas6 in renal cell carcinoma reflecting tumor advancement and survival. Clin Cancer Res 2009;15:4742–4749.
[37] **Zhang Z**, **Lee JC**, Lin L, Olivas V, Au V, LaFramboise T, et al. Activation of the AXL kinase causes resistance to EGFR-targeted therapy in lung cancer. Nat Genet 2012;44:852–860.
[38] Carrera Silva EA, Chan PY, Joannas L, Errasti AE, Gagliani N, Bosurgi L, et al. T cell-derived protein S engages TAM receptor signaling in dendritic cells to control the magnitude of the immune response. Immunity 2013;39:160–170.
[39] Bosurgi L, Bernink JH, Delgado Cuevas V, Gagliani N, Joannas L, Schmid ET, et al. Paradoxical role of the proto-oncogene Axl and Mer receptor tyrosine kinases in colon cancer. Proc Natl Acad Sci U S A 2013;110:13091–13096.
[40] Kariolis MS, Miao YR, Jones 2nd DS, Kapur S, Mathews II, Giaccia AJ, et al. An engineered Axl 'decoy receptor' effectively silences the Gas6-Axl signaling axis. Nat Chem Biol 2014;10:977–983.
[41] Uehara S, Gotoh K, Handa H, Maki Y. J Cancer Ther 2013;4:632–639.
[42] Schuppan D, Kim YO. Evolving therapies for liver fibrosis. J Clin Invest 2013;123:1887–1901.